Swing Up Control and Stabilization of the Pendubot

A Project Report

submitted by

SRINATH B

in partial fulfilment of the requirements

for the award of the degree of

MASTER OF TECHNOLOGY

DEPARTMENT OF ELECTRICAL ENGINEERING
INDIAN INSTITUTE OF TECHNOLOGY MADRAS

May 2016

THESIS CERTIFICATE

This is to certify that the thesis titled **Swing Up Control and Stabilization of the Pendubot**, submitted by **Srinath B**, to the Indian Institute of Technology, Madras, for the award of the degree of **Master of Technology**, is a bona fide record of the research work done by him under our supervision. The contents of this thesis, in full or in parts, have not been submitted to any other Institute or University for the award of any degree or diploma.

Dr. Arun D Mahindrakar
Research Guide
Associate Professor
Dept. of Electrical Engineering
IIT-Madras, 600 036

Place: Chennai

Date: 17th May 2016

ACKNOWLEDGEMENTS

I am greatly indebted to my guide, **Dr. Arun D Mahindrakar** for his valuable advice and timely help which helped me to complete the work.

ABSTRACT

KEYWORDS: Pendubot, Under-actuated system, Partial feedback linearization, Lyapunov function and Pole-placement.

Swing up control and stabilization of the Pendubot about the upright position is considered in this thesis. Pendubot is a two-link manipulator with a single actuator. The goal is to swing the pendubot from the stable downward position to the unstable up-right position and balance it there. This is achieved using two control strategies. Using swing up control, the Pendubot reach the close vicinity of the up-right position from the downward position. Once it is close to the upright position, the control is switched to balancing control for stabilizing the Pendubot about the upright position. Two swing up control strategies are presented here. First, Partial feedback linearization technique which introduce a double integrator system, is presented. Secondly, energy based approach using passivity property of the Penubobot is seen. For stabilization of the Pendubot about the unstable upright position, the nonlinear model of the Pendubot is linearized about the desired position and state feedback control law is designed to make the resulting system matrix Hurwitz using pole-placement method. Finally, the simulation and experiment results of the control strategies are presented.

TABLE OF CONTENTS

LIST OF TABLES

LIST OF FIGURES

ABBREVIATIONS

LQR Linear Quadratic Regulator

NOTATION

$\mathbb{R}^n$	n-dimensional real vector space
$\mathbb{R}^{m \times n}$	Set of $m \times n$ matrices with real entries
$\mathbb{S}^n$	n-dimensional unit sphere
V	Lyapunov function
A, B, K, M, C, G	Matrices with real entries

CHAPTER 1

Introduction

The Pendubot, a two-link robot manipulator with workspace in a vertical plane, was introduced by Daniel J. Block in his master's thesis [Block, 1996]. Pendubot is a variant of Acrobot (see Spong [1995]) with difference only in the actuation. The Acrobot has active elbow joint, where as, the Pendubot has active shoulder joint.

1.1 Pendubot

The Pendubot is a two link planar robot manipulator as shown in Figure 2.1. It comes under the class of under-actuated systems since it has less actuators than the number of degrees of freedom . The shoulder joint is active, where as, the elbow joint is passive providing unconstrained 360° rotation to link 2.

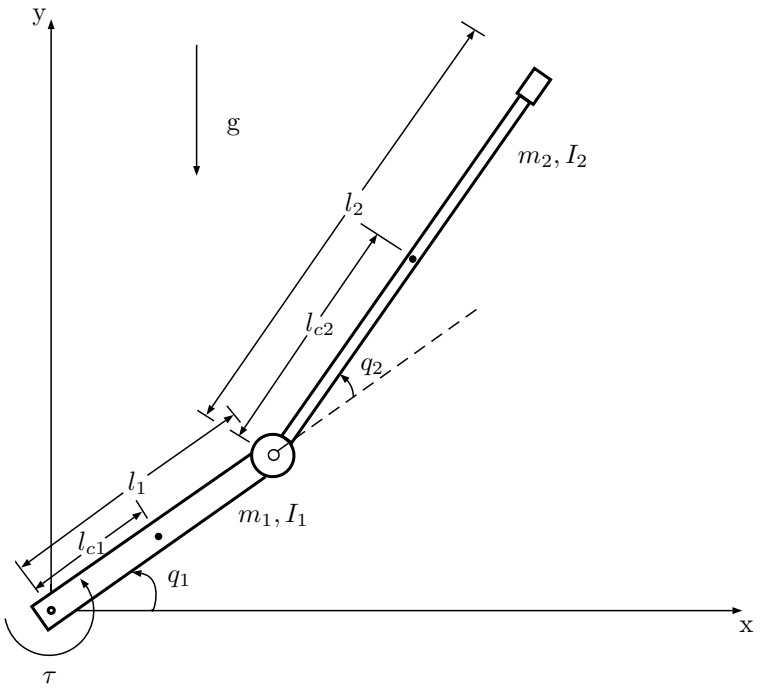

Figure 1.1: Pendubot Schematic

The mathematical model of the Pendubot is presented in [Block, 1996]. By virtue of passive elbow joint, the model has second order dynamic constraint on the states.

The Pendubot is a second order non-holonomic system because integrability condition on the constraint is not satisfied (see [Zhang and Tarn, 2002]). The Pendubot, being a nonholonomic system, satisfies the Brockett's necessary condition for smooth asymptotic stabilizability. However, Brockett's necessary condition will not be satisfied, if there are no gravitational terms in the mathematical model. In such cases, non smooth control has to be employed for asymptotic stabilization to the upright position.

1.2 Swing up control

Swing up control brings the Pendubot from the stable downward position to the unstable upright position. There exist many ways of achieving the swing up control as reported in [Block, 1996; Fantoni *et al.*, 2002; Consolini and Maggiore, 2011], but, in this thesis, only two distinct control strategies are considered.

First, partial feedback linearization technique in [Spong, 1995; Block, 1996] is considered. Due to under-actuated nature of the system, the system is not feedback linearizable. Hence, with partial feedback linearization either of the links response is linearized. If the upper arm is linearized by this technique, then it is called collocated linearization. In this case, there always exist partial feedback linearizing control law. On the other hand, if the lower arm is linearized, then it is called non-collocated linearization. In this case, partial feedback linearizing control exist only on certain condition. Secondly, energy based approach in [Fantoni *et al.*, 2002] is seen. In this approach, a candidate Lyapunov function using passivity property of the Pendubot is chosen. From the Lyapunov function, control law is picked such that the derivative of the Lyapunov function is negative semi-definite. There are variants of energy based approach (see [Gulan *et al.*]).

1.3 Stabilization of the Pendubot

Position stabilization scheme stabilizes the Pendubot about the unstable upright position using state feedback control. The nonlinear state space model presented in [Block, 1996] is linearized about the upright equilibrium point. Then a suitable feedback gain matrix is chosen such that the resulting system matrix is Hurwitz and also the stabiliza-

tion behavior is robust and satisfactory.

Due to the presence of gravitational terms in the Pendubot model, Brockett's necessary condition for smooth asymptotic stabilization to the equilibrium point is satisfied. If there is no gravitational terms in the mathematical model, then there exist no smooth feedback control law for asymptotic stabilization to the equilibrium point (see Zhang and Tarn [2002]). In such case, non smooth control law proposed in Zhang and Tarn [2002] has to be employed.

1.4 Organization of the dissertation

The organization of the dissertation is as follows

Chapter 2

The equation of motion of the Pendubot is presented. The states of the Pendubot are defined and state space model is derived subsequently. Later, the equilibrium points of the system are found and for each of the equilibrium points, stability property is given. The swing up control problem is presented and control laws for two distinct swing up control strategies are given. Finally, position stabilization problem is presented with the control law.

Chapter 3

The simulation and experimental results for each of the swing up control strategies along with position stabilization via state feedback control are provided.

Chapter 4

In the final chapter, concluding remarks are given.

Appendix A

Pendubot hardware and its program structure and flow are described. In addition, implementation details of the control and algorithm for states calculation are furnished.

Appendix B

Appendix B explains how the gains for each of the control laws were tuned.

CHAPTER 2

Swing Up Control and Stabilization of the Pendubot

In this chapter, the equation of motion of the Pendubot is presented. The states of the Pendubot are defined and state space model of the Pendubot is derived subsequently. Later, the equilibrium points of the system are found and for each of the equilibrium points, stability property is given. The swing up control problem is presented and control laws for two distinct swing up control strategies are given. In the end, stabilization of the Pendubot about the upright position is discussed.

2.1 Model of Pendubot

The Pendubot schematic is shown in Figure (2.1). The generalized coordinates q_1 and q_2 represent the angle between the horizontal plane and link 1 and the angle of link 2 relative to link 1. m_i, l_i, l_{ci}, I_i describe the mass, length, distance of center of mass from the pivot and moment of inertia about the center of mass of the link respectively. g, τ represent the acceleration due to gravity and torque acting at joint 1.

Lets assign $\tilde{q}_1 = q_1 - \frac{\pi}{2}$. Under the assumption of negligible friction at the joints, the equation of motion of the Pendubot follows,

$$M(q)\ddot{q} + C(q, \dot{q})\dot{q} + G = u \tag{2.1}$$

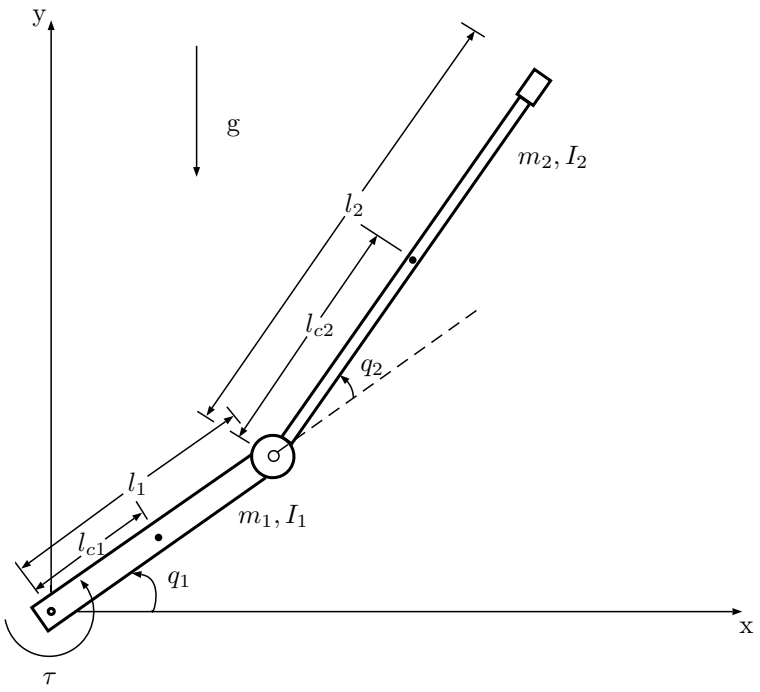

Figure 2.1: Pendubot Schematic

where,

$$
\begin{aligned}
q &= \begin{pmatrix} \tilde{q}_1 \\ q_2 \end{pmatrix}, \quad u = \begin{pmatrix} \tau \\ 0 \end{pmatrix}, \\
M(q) &= \begin{bmatrix} P_1 + P_2 + 2P_3 \cos q_2 & P_2 + P_3 \cos q_2 \\ P_2 + P_3 \cos q_2 & P_2 \end{bmatrix}, \\
C(q, \dot{q}) &= \begin{bmatrix} -P_3 \cos q_2 \, \dot{q}_2 & -P_3 \cos q_2 (\dot{q}_1 + \dot{q}_2) \\ P_3 \cos q_2 \, \dot{q}_2 & 0 \end{bmatrix}, \\
G(q) &= \begin{bmatrix} -P_4 \sin \tilde{q}_1 - P_5 \sin(\tilde{q}_1 + q_2) \\ -P_5 \sin(\tilde{q}_1 + q_2) \end{bmatrix}.
\end{aligned}
\tag{2.2}
$$

The parameters used in (2.2) are described below

$$
\begin{aligned}
P_1 &= m_1 {l_{c_1}}^2 + I_1 + m_2 {l_1}^2 \\
P_2 &= m_2 {l_{c_2}}^2 + I_2 \\
P_3 &= m_2 l_1 l_{c_2} \\
P_4 &= m_1 l_{c_1} + m_2 l_1 \\
P_5 &= m_1 l_{c_2}
\end{aligned}
\tag{2.3}
$$

In equation (2.1), $M(q)$ is the mass matrix , $C(q,\dot{q})\dot{q}$ is the vector containing the coriolis and centripetal terms, $G(q)$ contains the gravitational terms, u is the input vector. The Pendubot is a second order non-holonomic system, since the second order constraint on the states in (2.1) does not satisfy integrability condition (see [Zhang and Tarn, 2002]).

Solving for $\ddot{q}$ from equation (2.1) , we get

$$\begin{bmatrix} \ddot{q}_1 \\ \ddot{q}_2 \end{bmatrix} = M^{-1}\left[\begin{pmatrix} \tau \\ 0 \end{pmatrix} - C\dot{q} - G\right] \tag{2.4}$$

Let the states of the Pendubot be defined as $x = (x_1, x_2, x_3, x_4)^T \triangleq (\tilde{q}_1, q_2, \dot{q}_1, \dot{q}_2)^T$ where $x \in \mathbb{S}^2 \times \mathbb{R}^2$. The state space model of the Pendubot follows

$$\dot{x} = \begin{bmatrix} x_3 \\ x_4 \\ f_1(x) \\ f_2(x) \end{bmatrix} + g(x)\,\tau \tag{2.5}$$

where

$$\begin{bmatrix} f_1(x) \\ f_2(x) \end{bmatrix} = -M^{-1}[C\,\dot{q} + G] \tag{2.6}$$

$$g(x) = \begin{bmatrix} 0 \\ 0 \\ M^{-1}\begin{bmatrix} 1 \\ 0 \end{bmatrix} \end{bmatrix} \tag{2.7}$$

To find the equilibrium points of the system, equation (2.5) is equated to 0 with $\tau = 0$.

$$\begin{bmatrix} x_3 \\ x_4 \\ f_1(x) \\ f_2(x) \end{bmatrix} = 0 \tag{2.8}$$

Solving equation (2.8), we get four equilibrium points. The equilibrium points of the Pendubot are given in table 2.1.

Table 2.1: Equilibrium points of the Pendubot

Position	Description	Stability
$x_{up} = (0, 0, 0, 0)$	Up position for both the links	Unstable
$x_{down} = (\pi, 0, 0, 0)$	Down position for both the links	Stable
$x_{mid1} = (0, \pi, 0, 0)$	Up position for link 1. Down position for link 2	Stable
$x_{mid2} = (\pi, \pi, 0, 0)$	Down position for link 1. Up position for link 2	Unstable

Following sections describe how to stablize the Pendubot at x_{up} by swinging the linkage from x_{down}.

2.2 Swing up control

The swing up control strategy has to bring the Pendubot from stable downward position x_{down} to the neighbourhood of unstable upright position x_{top}. It is achieved by two different control strategies given below

(i) Partial feedback linearization

(ii) Energy based approach

2.2.1 Partial feedback linearization

The Pendubot is not feedback linearizable by virtue of its under-actuated characteristics. Hence, attempts are made to linearize the response of either of the links by partial feedback linearization technique [Spong, 1995]. This resulted in two controllers for the swing up control problem obtained by linearization of response of link 1 and link 2 separately. Lets derive the two control law,

The equation of motion of the Pendubot (2.1) can be rewritten as follows,

$$m_{11}\ddot{q_1} + m_{12}\ddot{q_2} + c_1(q, \dot{q}) + g_1(q) = \tau \tag{2.9}$$

$$m_{21}\ddot{q_1} + m_{22}\ddot{q_2} + c_2(q, \dot{q}) + g_2(q) = 0 \tag{2.10}$$

where,

$$\begin{aligned} m_{11} &= P_1 + P_2 + 2P_3 \cos q_2 \\ m_{12} &= P_2 + P_3 \cos q_2 \\ m_{21} &= m_{12} \\ m_{22} &= P_2 \end{aligned} \tag{2.11}$$

$$\begin{aligned} c_1(q, \dot{q}) &= -P_3 \cos q_2 (2\,\dot{q}_1 \dot{q}_2 + \dot{q}_2^2) \\ c_2(q, \dot{q}) &= P_3 \cos q_2\, \dot{q}_1 \dot{q}_2 \\ g_1(q) &= -P_4 \sin \tilde{q}_1 - P_5 \sin(\tilde{q}_1 + q_2) \\ g_2(q) &= -P_5 \sin(\tilde{q}_1 + q_2) \end{aligned} \tag{2.12}$$

Lets say, $\ddot{q}_1 = v$.

Solving equation (2.10) for $\ddot{q}_2$, we get

$$\ddot{q}_2 = -\frac{(m_{21} v + c_2(q, \dot{q}) + g_2(q))}{m_{22}} \tag{2.13}$$

τ is related to v as,

$$\tau = \left(m_{11} - m_{12} \frac{m_{21}}{m_{22}} \right) v + \left(c_1 - m_{12} \frac{c_2}{m_{22}} \right) + \left(g_1 - m_{12} \frac{g_2}{m_{22}} \right) \tag{2.14}$$

The control law (2.14) always exists to linearize the Pendubot partially, in view of m_{22} being bounded away from 0.

With

$$v = k_p\, q_1 + k_d\, \dot{q}_1, \tag{2.15}$$

τ gives corresponding signal that partially linearizes the Pendubot and performs PD control action for swinging up the Pendubot. However, appropriate choice of gains is required to meet the swing up control objective. This approach is called collocated linearization where the response of the actuated link is linearized.

Now, let $\ddot{q}_2 = v$.

Solving equation (2.10) for $\ddot{q}_1$, we get

$$\ddot{q_1} = -\frac{m_{22}v + c_2(q,\dot{q}) + g_2(q)}{m_{21}} \tag{2.16}$$

τ is related to v as,

$$\tau = \left(m_{12} - m_{11}\frac{m_{22}}{m_{21}}\right)v + \left(c_1(q,\dot{q}) - m_{11}\frac{c_2(q,\dot{q})}{m_{21}}\right) + \left(g_1(q) - m_{11}\frac{g_2(q)}{m_{21}}\right) \tag{2.17}$$

For existence of control law τ in (2.17), m_{21} should take non-zero value for all values of q_2. This condition is termed as *strong inertial coupling* in [Spong, 1995]. Strong inertial coupling condition imposes some restriction on the parameters of the Pendubot.

For $m_{21} > 0 \ \forall \ q_2$, the constraint (2.18) on the system parameters has to be satisfied.

$$m_2 \, {l_{c_2}}^2 + I_2 > m_2 \, l_1 \, l_{c_2} \tag{2.18}$$

This approach of partial feedback linearization is called non-collocated linearization since the non-actuated link i.e. link 2 response is linearized. Now, the next task is to chose v aptly such that the swing up control objective is met. For further details in choosing the outer loop control term v see [Spong, 1995]. In this thesis, collocated linearization alone is considered and implemented on the Pendubot setup.

2.2.2 Energy based approach

The swing up control of the Pendubot using partial feedback stabilization in [Block, 1996] did not provide stability analysis. Further, the torque is required to be large so that the Pendubot reaches the close vicinity of upright position in the first swing itself. On the other hand, for energy based approach, complete stability analysis is provided based on Lyapunov theory in [Fantoni *et al.*, 2002]. Moreover, the energy pumped to the Pendubot is relatively less than former case and it comes at the cost of time taken to reach the close vicinity of the upright position.

The total energy of the Pendubot is given by

$$E(q,\dot{q}) = \frac{1}{2}\dot{q}^T M(q)\dot{q} + P_4 g \cos q_1 + P_5 g \cos(q_1 + q_2) \tag{2.19}$$

When the Pendubot is at x_{top}, the total energy is

$$E_{top} = (P_4 + P_5)g \tag{2.20}$$

Fantoni *et al.* [2002] defined the candidate Lyapunov function as

$$V(q, \dot{q}) = \frac{k_E}{2}\tilde{E}(q, \dot{q})^2 + \frac{k_D}{2}\dot{\tilde{q}}_1^2 + \frac{k_P}{2}\tilde{q}_1^2 \tag{2.21}$$

where $\tilde{E} = E - E_{top}$ and k_E, k_D, k_P are strictly positive constant satisfying

$$\frac{k_D}{k_E} > 2P_1(P_4 + P_5)g \tag{2.22}$$

and showed if the constraints (2.23)

$$\begin{aligned} |\tilde{E}(0)| < c &:= min(2P_4 g, 2P_5 g) \\ V(0) &\leq \frac{1}{2}k_E c^2 \end{aligned} \tag{2.23}$$

hold for initial condition $q(0)$ and $\dot{q}(0)$ for some ϵ, then the solution of the closed-loop system (2.5) with the control law

$$\tau = \frac{-k_D F(q, \dot{q}) - (P_1 P_2 - P_3^2 \cos^2 q_2)(\dot{q}_1 + k_P \tilde{q})}{(P_1 P_2 - P_3^2 \cos^2 q_2)k_E \tilde{E} + k_D P_2} \tag{2.24}$$

where

$$\begin{aligned} F(q, \dot{q}) = P_2 P_3 \sin q_2 (\dot{q}_1 + \dot{q}_2)^2 + P_3^2 \cos q_2 \sin q_2 \, \dot{q}_1^2 + \\ P_2 P_4 \, g \cos \tilde{q}_1 - P_3 P_5 \, g \cos q_2 \sin(q_1 + q_2) \end{aligned} \tag{2.25}$$

converges to the invariant set M given by the homoclinic orbit

$$\frac{1}{2}P_2 \dot{q}_2^2 = P_5 g(1 - \cos q_2) \tag{2.26}$$

with $(\tilde{q}_1, \dot{q}_1) = (0, 0)$ and the interval $(\tilde{q}_1, \dot{q}_1, q_2, \dot{q}_2) = (-\epsilon, 0, \epsilon, 0)$, where $|\epsilon| < \epsilon^*$ and ϵ^* is arbitrarily small. The convergence of the closed loop system to the homoclinic orbit solves the swing up control problem. The condition (2.22) rules out singularities in the control law (2.24). Using the control law (2.24), the Pendubot can stuck at any of the equilibrium points of the Pendubot and it can avoided if the condition (2.23) is

satisfied.

The constraints (2.22) and (2.23) are exploited to arrive at k_P, k_D and k_E for the swing up control.

2.3 Stabilization of the Pendubot

The swing up control brings the Pendubot close to the upright positon and then the control law is switched to the stabilizing control for stabilization about x_{top}. In this thesis, state feedback control is considered to stabilize the Pendubot about x_{top}. The nonlinear model of the Pendubot (2.5) is linearized about x_{top} and the linearized system is represented by

$$\dot{x} = Ax + B\tau \tag{2.27}$$

where

$$\begin{aligned} A &= \begin{bmatrix} 0 & 0 & 1 & 0 \\ 0 & 0 & 0 & 1 \\ \frac{(P_2P_4-P_5P_3)g}{(P_1P_2-P_3)^2} & \frac{-P_3P_5g}{(P_1P_2-P_3)^2} & 0 & 0 \\ \frac{(P_1+P_3)P_5g-(P_2+P_3)P_4g}{(P_1P_2-P_3)^2} & \frac{(P_1+P_3)C_5g}{(P_1P_2-P_3)^2} & 0 & 0 \end{bmatrix} \\ B &= \frac{1}{(P_1P_2-P_3)^2} \begin{bmatrix} 0 \\ 0 \\ P_2 \\ -P_2-P_3 \end{bmatrix} \end{aligned} \tag{2.28}$$

For the system parameters of the Pendubot in table (A.1), equation (2.28) becomes

$$A = \begin{bmatrix} 0 & 0 & 1 & 0 \\ 0 & 0 & 0 & 1 \\ 118.7040 & -52.0195 & 0 & 0 \\ -133.4012 & 130.0511 & 0 & 0 \end{bmatrix}$$

$$B = \begin{bmatrix} 0 \\ 0 \\ 2934.5911 \\ -4528.5202 \end{bmatrix} \tag{2.29}$$

The controllability matrix of system (2.27) is constructed

$$\begin{bmatrix} B & AB & A^2B & A^3B \end{bmatrix} = \begin{bmatrix} 0 & 0.0293 & 0 & 5.8392 \\ 0 & -0.0453 & 0 & -9.8042 \\ 0.0293 & 0 & 5.8392 & 0 \\ -0.0453 & 0 & -9.8042 & 0 \end{bmatrix} \tag{2.30}$$

and the rank of the controllability matrix is found to be 4. Hence, the system (2.27) is completely controllable.

For state feedback control, the control law follows

$$\tau = -Kx \tag{2.31}$$

where $K \in \mathbb{R}^{4\times 1}$.

The gain matrix K is chosen using pole-placement method for asymptotic stabi-

lization to x_{top}. Pole-placement method provides a constructive way to tune the gains. Asymptotic stabilization to x_{top}, provided $A-BK$ is hurwitz and the system (2.27) is in the region of attraction of the stabilizing control at time of switching, is the case only in simulation since the nonlinearities associated with the actuator such as motor friction, backlash etc. does not come in the simulation model. Therefore, when it comes to implementation, the mere choice of the gain matrix K such that $A-BK$ is hurwitz, alone is not sufficient. The poles of the closed loop system have to be chosen such that they give desired stabilization response. Appendix B gives details of desired stabilization behavior. In our case, we choose the gains by tuning through experiments.

CHAPTER 3

Simulation and Experiment results

3.1 Experiment setup

The Pendubot setup is shown in Figure (3.1). The hardware, program flow and structure of the Pendubot are provided in Appendix (A). The procedure adopted for tuning the gains of each of the control laws is detailed in Appendix (B).

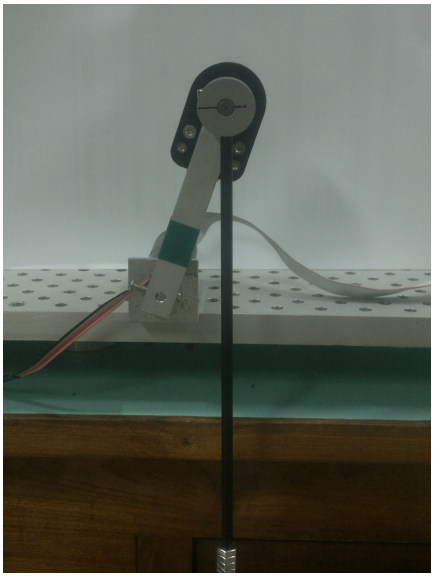

Figure 3.1: Pendubot setup

The encoder cable from joint 2 is routed as shown in Figure. This ensures the cable does not move significantly over repeated experiments. The cable routing is important because the opposing torque produced by the cable is not negligible compared with the operating range of the Pendubot. This is found by observing change in behavior of the Pendubot for different cable positions. By fixing the cable position, opposing torque due to the cable is made constant. Thereby, repeatability of the experiments is increased.

3.2 Simulation and Experiments

Experiment 1

In this experiment, the Pendubot is set into swing up motion by Partial Feedback Linearization technique and stabilization of the Pendubot is achieved using state feedback control. The control strategy switch from partial feedback linearization to state feedback control, if the condition (3.1) is satisfied.

$$|\tilde{q}_1| < 10^{\circ} AND |q_2| < 15^{\circ} \tag{3.1}$$

The bound on $\tilde{q}_1$ and q_2 is arrived by simulation. Though the bound on $\dot{q}$ is not explicitly given in the switching condition, it is taken care by appropriate choice of control parameters of the swing up control (see Appendix B). The gains of the control laws eqs. (2.15) and (2.31) are chosen to be $k_p = 600$, $k_d = 70.75$, $k_1 = -1.9862$, $k_2 = -1.7129$, $k_3 = -0.3207$ and $k_4 = -0.2343$. The initial condition is $(\tilde{q}_1, \dot{q}_1, q_2, \dot{q}_2) = (-\pi, 0, 0, 0)$. Figure 3.2 shows the time response of the states and control input and the energy profile of the Pendubot.

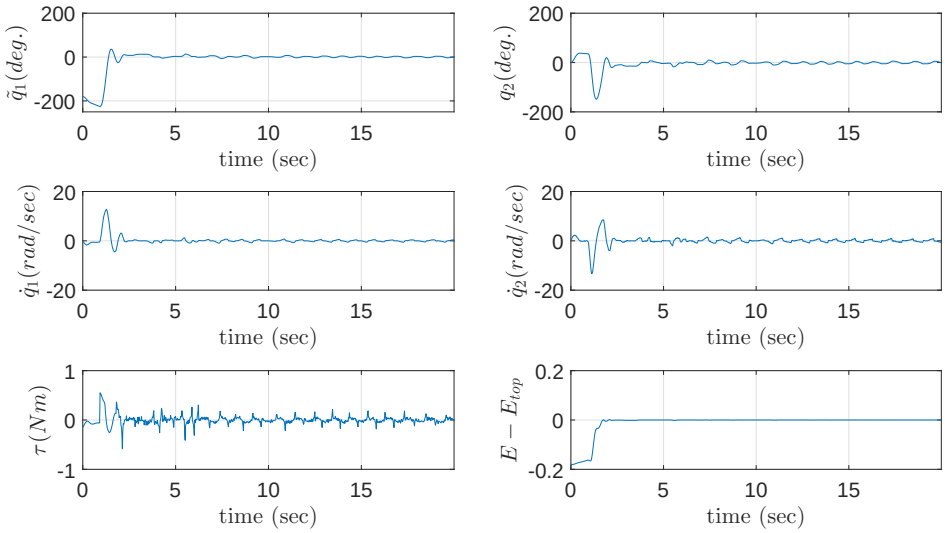

Figure 3.2: Time response of states and control input and Energy profile

The plot of $\tilde{q}_1$ shows the Pendubot first move in one direction and then the swing up control 2.14 takes over to bring the Pendubot close to x_{top}. This is done to ensure

that the Pendubot reach the upright position in the swing up control. The spike in τ at approximate $2\,\mathrm{sec}$ is due to switching of control to state feedback control. As a result of switching, $(q, \dot{q})$ gets closer to $x_{top} = (0, 0, 0, 0)$. Note that states $(q, \dot{q})$ do not converge to x_{top}. It stays within a open ball of radius $\epsilon > 0$ with center x_{top}. This is because of friction at joint 1, a limit cycle is introduced at x_{top}.

Experiment 2

Energy based approach is used to swing up the Pendubot. The swing up control does not bring the Pendubot to the region of attraction of state feedback control with gain K used in Experiment 1. Hence, the gain matrix $\bar{K}$ is chosen such that the Pendubot can be brought to its region of attraction by the swing up control. With gain matrix $\bar{K}$, the Pendubot is taken to the region of attraction of state feedback control with gain K which has good stabilizing characteristics. Once it has reached the region of attraction, the control strategy is switched to $\tau = -K'x$. Algorithm 1 explains the switching of control strategy.

Algorithm 1 Control switch algorithm

Require: states of the Pendubot $(q, \dot{q})$

procedure CTRLSW($\tilde{q}_1, \dot{q}_1, q_2, \dot{q}_2$)
  if $|\tilde{q}_1| < 35^\circ$ And $|q_2| < 50^\circ$ And $|\dot{q}_1| < 0.01$ And $|\dot{q}_2| < 0.25$ **then**
    $sw \leftarrow 1$
    $u \leftarrow -\bar{K}'x$
  end if
  if $|\tilde{q}_1| < 5^\circ$ And $|q_2| < 5^\circ$ And $|\dot{q}_1| < 0.01$ And $|\dot{q}_2| < 0.005$ And $sw == 1$ **then**
    $u \leftarrow -K'x$
  end if
end procedure

The gains of the control law (2.24) are chosen to be $k_P = 0.08$, $k_D = 0.075$ and $k_E = 3000$. The gains of state feedback control (2.31) are chosen to be $k_1 = -1.9862$, $k_2 = -1.7129$, $k_3 = -0.3207$, $k_4 = -0.2343$,$\bar{k}_1 = -1.75$, $\bar{k}_2 = -1.6123$, $\bar{k}_3 = -0.5203$ and $\bar{k}_4 = -0.4015$ is used. The initial condition is $(\tilde{q}_1, \dot{q}_1, q_2, \dot{q}_2) = (11^\circ, 169^\circ, 0, 0)$.

When link 1 is pushed from one side as part of swing up maneuver, the torque (lets say counter torque) required to stop link 1 is high due to friction at joint 1. Thus, link 1 moves quite far compared to $\tilde{q}_1$ in simulation for the counter torque to be high enough

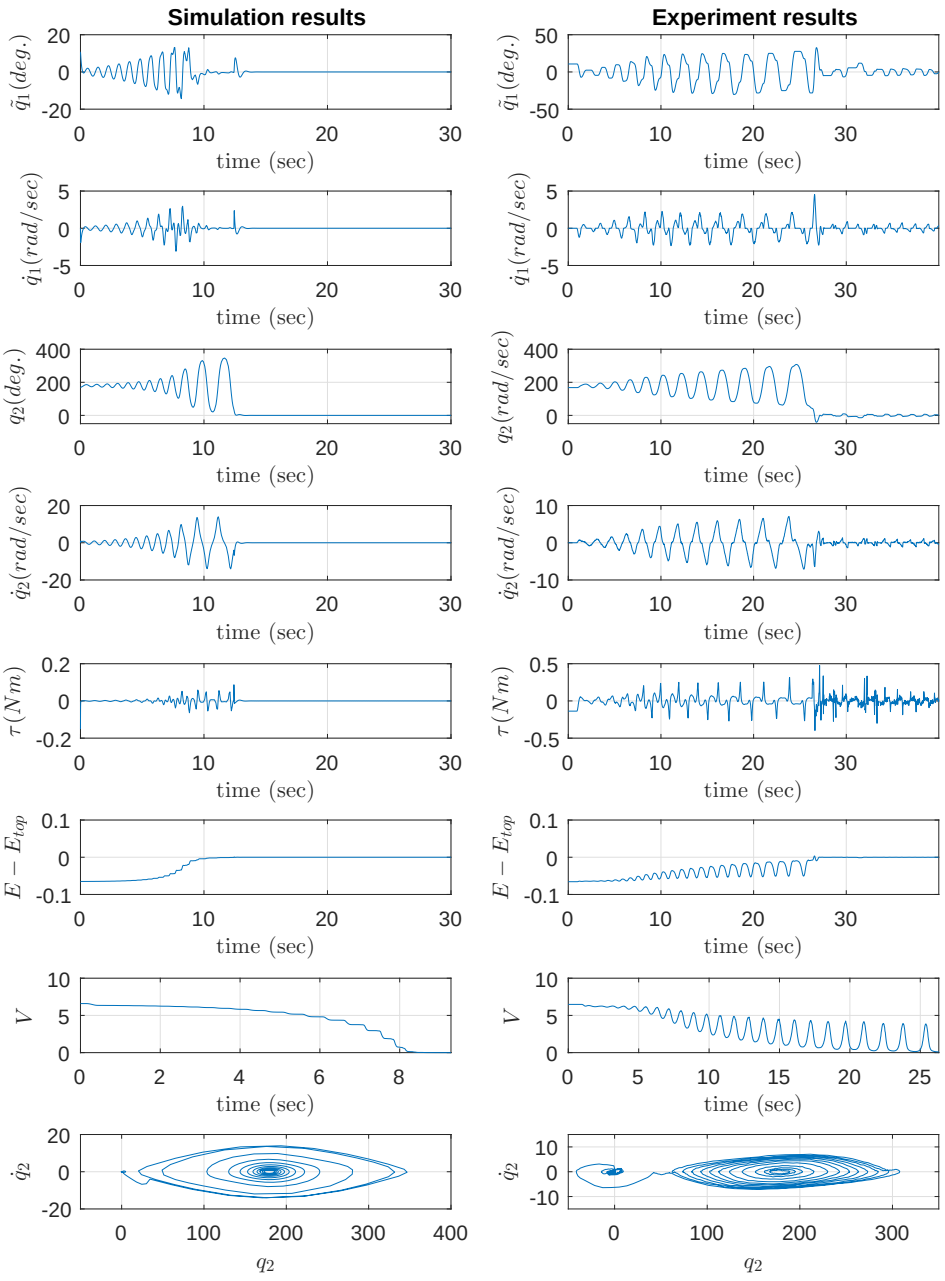

Figure 3.3: Time response of states, control input, Energy function $E - E_{top}$, Lyapunov function V and phase portrait of $(q_2, \dot{q}_2)$

to stop its motion. Thats why in each half cycle $\tilde{q}_1$ and $\dot{q}_1$ are relatively high than their counterparts in simulation. Such high torque also moves link 1 in opposite direction by the act of stopping it. This led to decrease in energy of the system as seen in the energy function $E - E_{top}$ plot. The same can be attributed to the decrease in the Lyapunov

function V as it contains the energy term. In the next swing up maneuver, link 2 moves less compared to its counterpart in simulation because it has to make up for the energy loss in the previous swing up. The energy function $E - E_{top}$ starts increasing due to the next swing up maneuver and continues to be increasing till the counter torque act on link 1 to move towards $\tilde{q}_1 = 0$.

As this repeats for every swing up action, the regular increase and decrease in the energy function $E - E_{top}$ and lyapunov function V are noticed. The phase portrait of $(q_2, \dot{q}_2)$ shows the convergence of the system to homoclinic orbit (2.26). Figure 3.4 shows disturbance rejection characteristics of state feedback control.

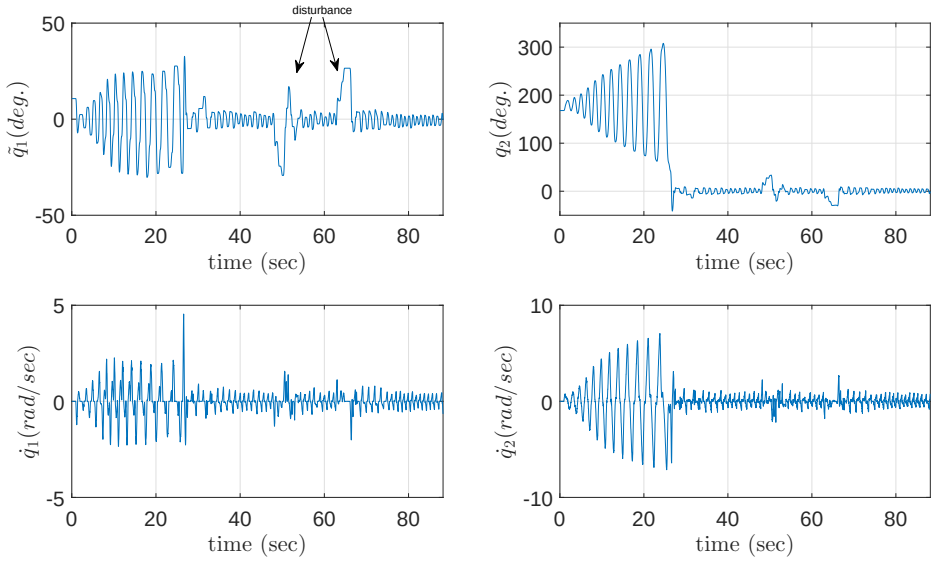

Figure 3.4: Disturbance rejection characteristics of state feedback control

CHAPTER 4

Conclusion

In this thesis, swing up control and stabilization of the Pendubot about the upright position is presented. Two different control strategies are used to achieve the objective. For swing up control, two control schemes are adopted, namely, Partial feedback linearization and Energy based approach using passivity property. The nonlinear model of the system is linearized about the upright position and state feedback control is designed for stabilization about the upright position. The simulation and experimental results are provided. The reason for the mismatch in the simulations and experiments are explained.

APPENDIX A

Description of Pendubot Hardware and Program

A.1 Hardware

The Pendubot setup is shown in Figure A.1. The links are made out of aluminum. The actuated joint is driven by Maxon brushed DC motor of part number 397019 which come with an encoder of resolution 512 counts per revolution(CPR). The link 1 houses an optical encoder which provide unconstrained 360° revolution to the link 2.

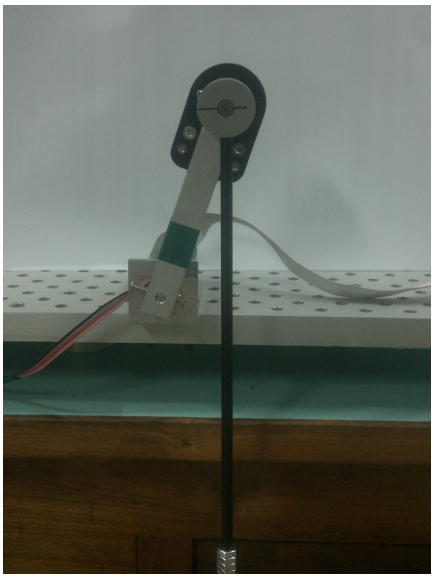

Figure A.1: Pendubot setup

A schematic of Pendubot is shown in Figure A.2 . It contain components which process the optical encoder signals to get the states which is used to decide the control action. The brushed dc motor is driven by a PWM signal using Maxon 4-Q-DC Servoamplifier ADS 50/5. Maxon shunt regulator DSR 70/30 is used with the servoamplifier to limit its supply voltage level during long braking process. Xbee module is used to transmit all the states of the Pendubot to the PC.

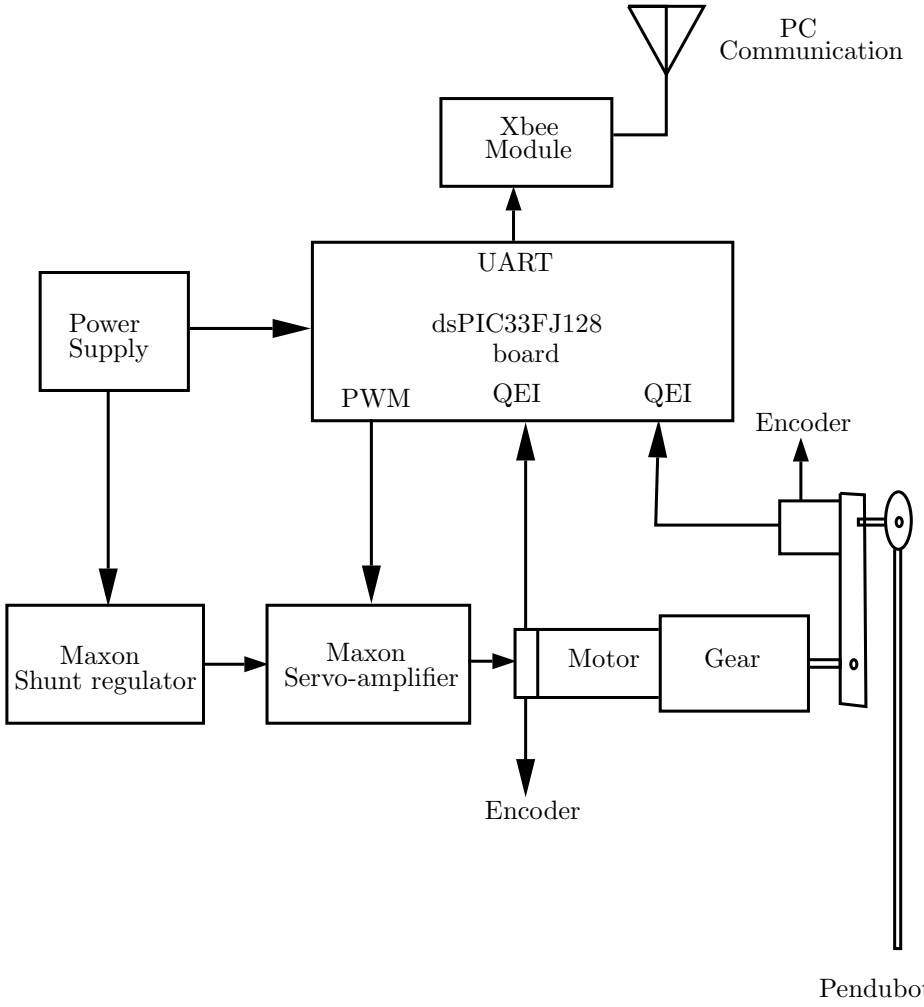

Figure A.2: Schematic diagram of the Pendubot

A.2 Program description

A.2.1 Main program

In main program, Microchip dsPIC's features like PWM module, QEI module, timer module and UART module are initialized along with clock oscillator. Once initialization of all the modules are done, the timer is started. Then the controller enters into the infinite loop, commonly called wait state where it continues to stay till the interrupts arrive. When an interrupt occurs, the associated interrupt service routine is executed. After the routine is serviced, the controller returns back to the wait state. And the cycle repeats. This is depicted in Figure (A.3).

The initialization of dsPIC modules is described below in detail.

1. The internal FRC oscillator is set as clock source for dsPIC. It is used with

PLL to obtain high operating frequency. The system clock frequency is set to 79.2275 MHz. Watchdog timer, power-up timer and code protect feature are turned off.

2. All analog-to-digital input pins are configured as digital input pins. QEI, PWM and UART module are assigned input and output pins.

3. PWM module is configured to operate in free running mode and its frequency is fixed at 1.2 kHz approximately. PWM I/O pin pair is assigned in independent output mode.

4. Digital noise filter is enabled in QEI module with $1:16$ digital filter clock divide and quadrature encoder interface mode enabled ($\times 4$) with position reset on match with maximum count register MAXxCNT.

5. In UART module, baud rate is set at 38400. The module is configured to generate a transmission interrupt when the last transmission is over and all the transmit operation is completed. In idle state, the transmit pin TX is set to be high.

6. Timer module is assigned to use instruction cycle clock as its source clock with interrupt period of 4.9 ms (or 204 Hz) roughly.

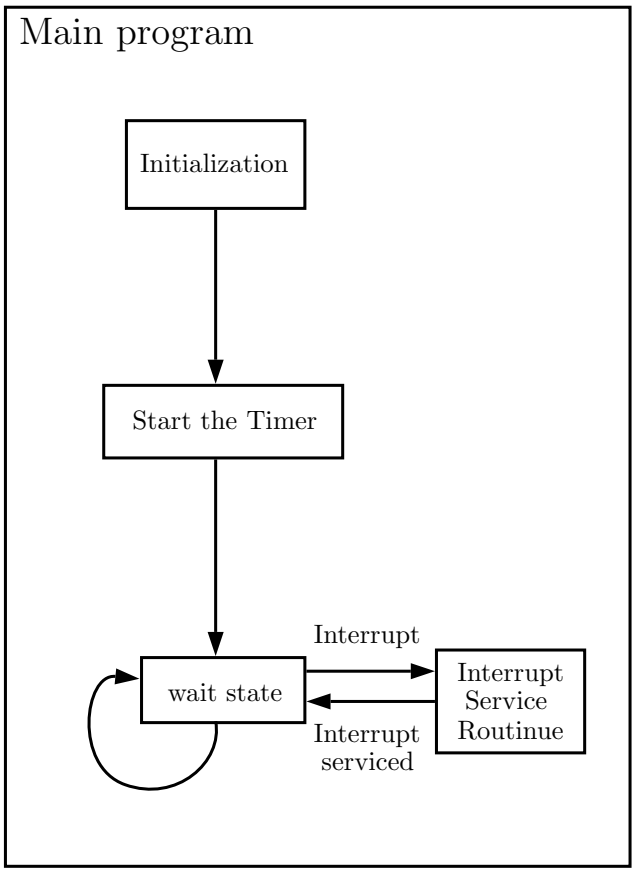

Figure A.3: Code flow in main program

A.2.2 Interrupt Service Routines

When an interrupt occur, interrupt service routine, shortly ISR, associated with it is executed. There are two interrupts used in the program, namely, timer interrupt and UART transmit interrupt . The work done by the ISR of the interrupts is given below

Timer interrupt

Timer interrupt acquires the encoder counts and processes them to reduce the effects of backlash in $(\tilde{q}_1, \dot{q}_1)$ and for smooth estimation of $\dot{q}$. Once the states are found, control function is executed. It calculates the torque to be applied from the states and later the torque calculated is converted to voltage using motor dynamics. In the end, states transmission is initiated with $\tilde{q}_1$ being transmitted.

UART transmit interrupt

After the transmission of state $\tilde{q}_1$ is done, UART transmit interrupt is generated. Interrupt service routine is programmed such that it continues to transmit the states till all the states are transmitted. This is depicted in Figure A.4.

States calculation

The states $(\theta, \dot{\theta})$ are calculated using the optical encoders at joint 1 and joint 2. The encoders, used in the setup, are incremental type, generating quadrature type signals A and B of varying width depending on the speed of rotation. The signals are processed by QEI module of dsPIC to give relative position in terms of counts. Due to gearhead arrangement of the brushed dc motor at joint 1, $(\tilde{q}_1, \dot{q}_1)$ are highly susceptible to errors. To minimize the error introduced by backlash, anti-backlash filter in [Muralidharan, 2014] is used, considering static backlash model presented in [Khalil, 1996].

We arrive at absolute angular position q by calculating the angular velocity from the encoder counts, integrating it over the sampling time and adding it with previous position.

$$q(n) = q(n-1) + \int_0^{t_s} \dot{q}(n)\, t = q(n-1) + \dot{q}(n) \times t_s \tag{A.1}$$

This method necessitates the estimation of angular velocity $\dot{\theta}_1$ from the encoder counts. Since position measurement is deteriorated by quantization error, estimation

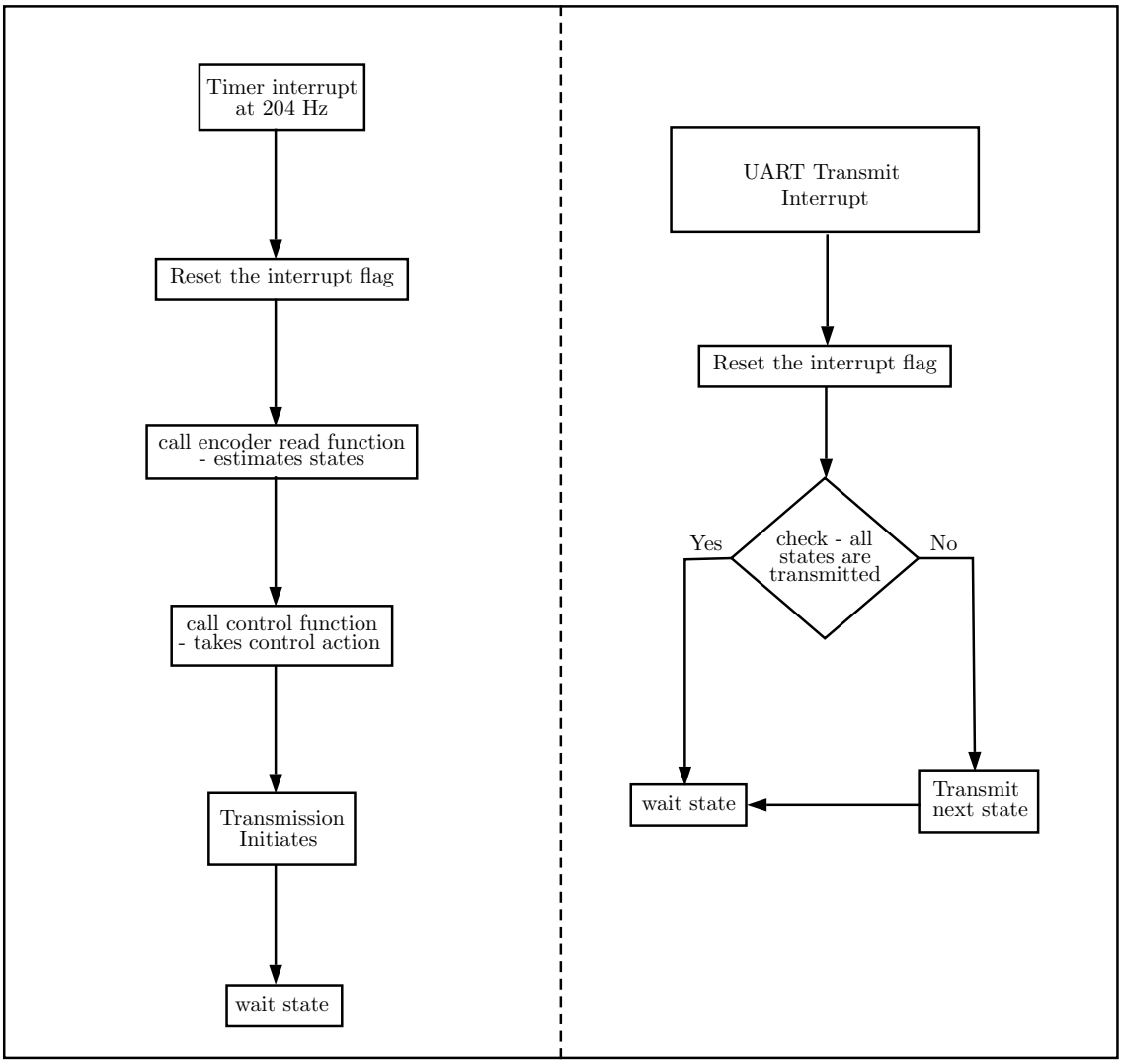

Figure A.4: Code flow in interrupt routines

of velocity by numerical differentiation may further worsen the signal to noise ratio. Hence, smoothing filter proposed in [Merry *et al.*, 2010] is used to obtain smooth estimate of velocity, which is essentially fitting a low-order polynomial to the encoder counts by least square fit and differentiating polynomial with the least square fitted coefficients to get velocity.

Let m be the order of the fit, n be the number of encoder counts used, $(p_1, p_2, \cdots, p_m)$ be the coefficients of the polynomial to be estimated and $x_i|_1^n$ be the encoder count at the time instant $t_i|_1^n$. Here, t_n is the present time instant. Lets define $A \in \mathbb{R}^{n \times m}$, $P \in \mathbb{R}^m$ and $B \in \mathbb{R}^n$ as follows,

$$A = \begin{bmatrix} t_1^m & t_1^{m-1} & \cdots & t_1 \\ \vdots & \vdots & & \vdots \\ t_{n-1}^m & t_{n-1}^{m-1} & \cdots & t_{n-1} \\ t_n^m & t_n^{m-1} & \cdots & t_n \end{bmatrix}, \tag{A.2}$$

$$P = \begin{bmatrix} p_m & p_{m-1} & \cdots & p_1 \end{bmatrix}^T, \tag{A.3}$$

$$B = \begin{bmatrix} x_1 & x_2 & \cdots & x_n \end{bmatrix}^T. \tag{A.4}$$

For least squares method, n has to be greater than m and the equation to be solved for P is given below

$$AP = B \tag{A.5}$$

The coefficients of the polynomial are computed using least square method as

$$P = (A^T A)^{-1} A^T B \tag{A.6}$$

Since velocity has to be known at t_n, the polynomial is extrapolated to t_n time instant with the fitted polynomial coefficients to get estimated position and estimated velocity as

$$\begin{aligned} \hat{x}(t)|_{t=t_n} &= p_m {t_n}^m + p_{m-1} {t_n}^{m-1} + \cdots + p_1 t_n \\ \hat{\dot{x}} &= \dot{\hat{x}} \end{aligned} \tag{A.7}$$

Once the velocity is estimated, it is filtered with chebyshev type-II filter with cutoff frequency $\omega_f = 60$ Hz. The cutoff frequency is chosen to be sufficiently larger than the system bandwidth ω_b so that the effect of extra phase lag of the filter is relatively small in the system behavior. The sampling rate ω_s is also chosen sufficiently large than system bandwidth , roughly $20\,\omega_b$, as mentioned in van der Laan [1995] so that there is 90% suppression at $\frac{\omega_s}{2}$. As a result, anti-aliasing filter can be omitted from filter design. The algorithm for angular velocity and position estimation is given in 2. In algorithm 2,

the time instants of the encoder counts $t_i|_1^n$ is set $i|_1^n$ and angular velocity is calculated in counts per sample time. Using sample time and encoder resolution, it is converted to radian per second.

Algorithm 2 Algorithm for angular velocity and position estimation

Require: sampling time t_s, Gear ratio N, Encoder resolution enc_{res}, encoder count x at present instant t_n, encoder count x_{prev} at previous instant t_{n-1} , joint angle at previous instant θ_{prev}, numerical difference of encoder counts at previous instant Δx_{prev}, stock of backlash compensated encoder counts over n period $\bar{X}$ and stock of backlash compensated ΔX over n period X'. Initially $x_{prev}, \theta_{prev}, \Delta x_{prev}, \bar{X}, X'$ are assigned 0.

procedure ENCREAD($x, \theta_{prev}, x_{prev}, \Delta x_{prev}, X'$)

$\Delta x \leftarrow x - x_{prev}$

if ▷ Backlash Compensation

  $(\Delta x > 0$ And $\Delta x_{prev} < 0)$ Or

  $(\Delta x < 0$ And $\Delta x_{prev} > 0)$ Or

  $(\Delta x \neq 0$ And $\Delta x_{prev} = 0)$ **then**

    $x'_n \leftarrow 0$

else

    $x'_n \leftarrow \Delta x$

end if

for $j \leftarrow 1$ to n **do** ▷ Construction of backlash compensated encoder counts x over m time period

  if $j = 1$ **then**

    $\bar{x}_j \leftarrow x'_j$

  else

    $\bar{x}_j \leftarrow x'_j + \bar{x}_{j-1}$

  end if

end for

$P \leftarrow (A^T A)^{-1} A^T \bar{X}$ ▷ coefficients of the polynomial calculation

$\hat{x}(n)|_{n=i} \leftarrow p_m * i^m + p_{m-1} * i^{m-1} + p_{m-2} * i^{m-2} + \ldots + p_1 * i$

$\hat{\dot{x}} \leftarrow \hat{\dot{x}}$ ▷ estimate of velocity

$\hat{\dot{\theta}} \leftarrow \hat{\dot{x}} * 2\pi/(t_s * N * enc_{res})$ ▷ Conversion from counts/t_s to rad/sec

for $j \leftarrow 1$ to $n - 1$ **do**

  $x'_j \leftarrow x'_{j+1}$

end for

$\hat{\theta} \leftarrow \hat{\theta}_{prev} + \hat{\dot{\theta}} * t_s$ ▷ Position estimate by deadreckoning

if $\hat{\theta} > 2\pi$ **then** ▷ Wrapping θ between 0 and 2π

  $\hat{\theta} \leftarrow \hat{\theta} - 2\pi$

end if

return $(\hat{\theta}, \hat{\dot{\theta}})$

end procedure

The states $(q, \dot{q})$ are validated by moving the links from a known position and stopping at the same position (see Figure A.5 and A.6). Figure A.7 shows the evolution of states $(q, \dot{q})$ due to free fall from x_{top} and as expected it reached stable equilibrium point x_{down}.

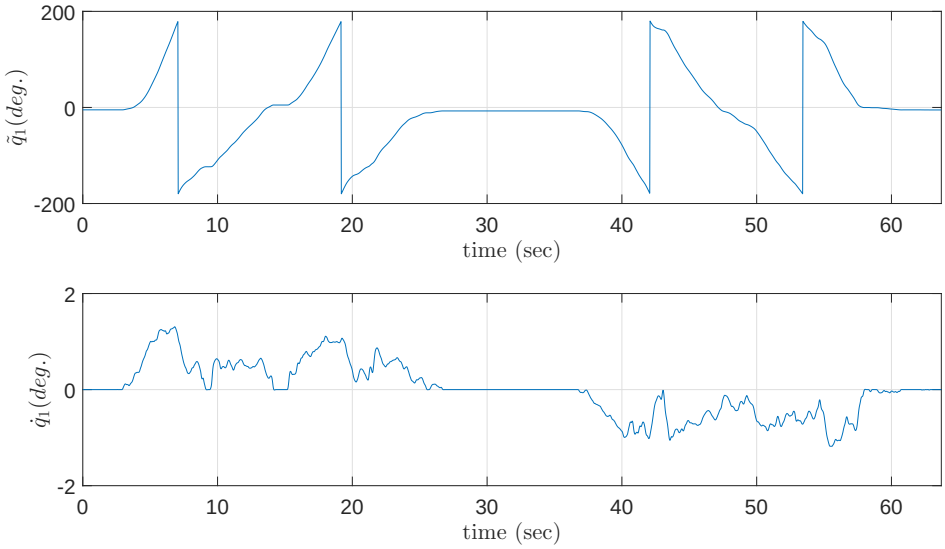

Figure A.5: Validation of $\tilde{q}_1$

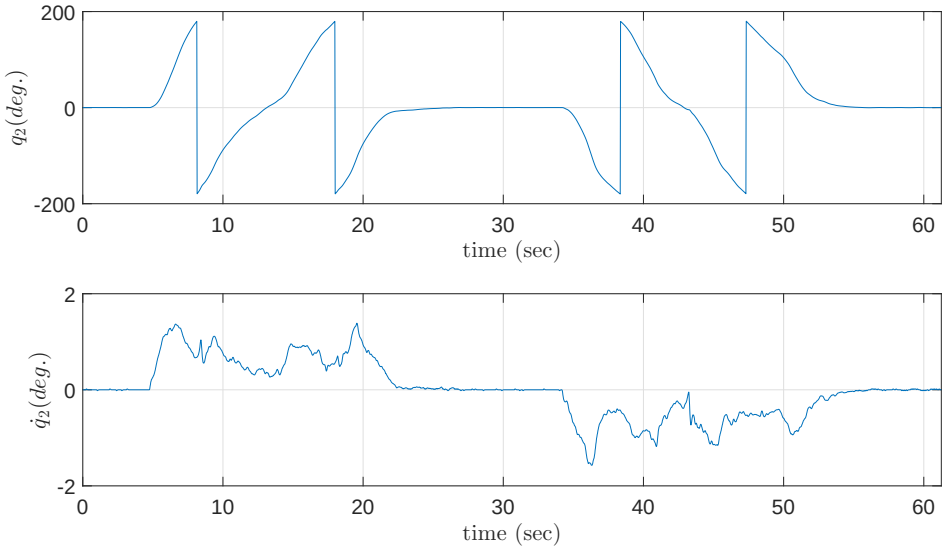

Figure A.6: Validation of q_2

Voltage calculation

Once the states are determined, control function computes the torque to be applied. In the case of non-linear control law, system parameters are required along with the states in torque calculation. The computed system paramters of the Pendubot are given in the table A.1.

The torque calculated is converted to voltage (A.8) using motor parameters such as back-emf constant k_b, gear ratio N, terminal resistance R_m, torque constant k_t, terminal

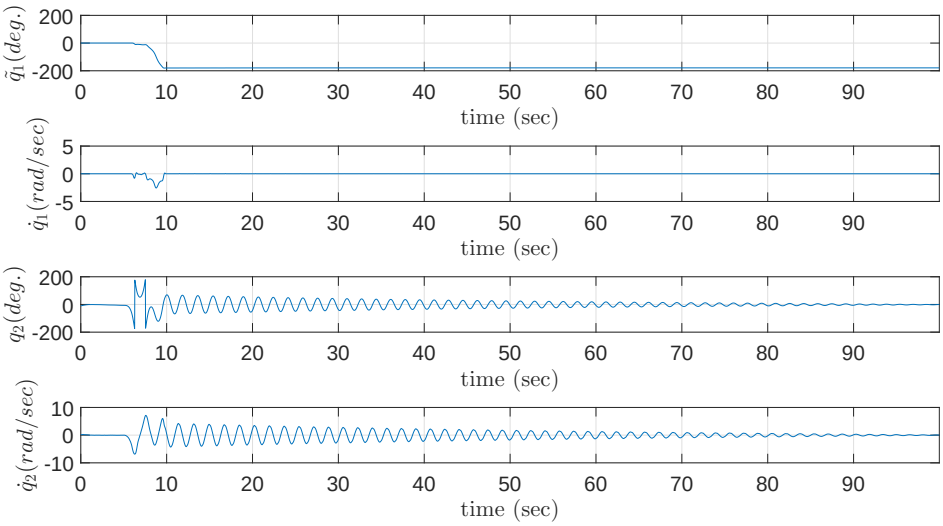

Figure A.7: Evolution of states $(q, \dot{q})$ due to free fall from x_{top}

Table A.1: System paramters

System parameter	Value
C_1	5.3419×10^{-04}
C_2	6.5564×10^{-04}
C_3	3.5611×10^{-04}
C_4	5.932×10^{-03}
C_5	3.328×10^{-03}

inductance L_m and motor states like angular velocity $\dot{\theta}_1$ and current i_m. Their values are $k_b = 2.75\, mV/rpm$, $N = 29$, $R_m = 33.3\,\Omega$, torque constant $k_t = 26.2\, mNm/A$.

$$V_m = k_b N \dot{\theta}_1 + \frac{R_m \tau}{k_t N} + L_m \frac{di_m}{dt} \tag{A.8}$$

For Maxon brushed DC motor, terminal inductance is very low so the voltage contribution by the last term is negligible. Therefore, it can neglected in the voltage calculation.

APPENDIX B

Gain tuning

The selection of gains of the control law is important for meeting the requirements of the desired behavior. In this section, we will detail how the gains are arrived for each of the control laws.

B.1 Partial feedback linearization

Here, the control law with outer PD control loop follows

$$\tau = \left(m_{11} - m_{12}\frac{m_{21}}{m_{22}}\right)v + \left(c_1 - m_{12}\frac{c_2}{m_{22}}\right) + \left(g_1 - m_{12}\frac{g_2}{m_{22}}\right) \tag{B.1}$$

where $v = k_p(0 - \tilde{q}_1) + k_d(0 - \dot{q}_1)$

Partial feedback linearization technique brings the Pendubot to the neighbourhood of x_{top} by linearizing the response of link 1. Once the Pendubot has come closer to the upright position, the control strategy is switched to state feedback control. However, if the links reach the region with high $\dot{q}$, then the switch to the stabilizing controller will produce instant high torque to counter the fast moving links which, in turn, can destabilize the system. This is because the Pendubot has not entered the basin of attraction of the stabilizing controller.

Therefore, there should be a constraint on angular velocities of the links $\dot{q}$ to guarantee asymptotic stabilization to the equilibrium point. The constraint $\|\dot{q}\| < 1$ is fixed by trail and error method in simulation. Table B.1 shows gain tuning rules adopted to bring the Pendubot to neighbourhood of the upright position with the constraint on $\dot{q}$ satisfied.

A good approach is to fix any one of the control parameters and tune the other depending upon the system response. In our case, k_p is fixed and k_d is tuned iteratively.

Table B.1: Tuning procedure for Partial feedback linearization

System response	Tuning	
	k_p	k_d
The Pendubot reach the upright position with high $\dot{q}$	decrease	increase
The Pendubot doesn't reach the upright position	increase	decrease

B.2 State feedback control

As stated in Chapter 2, asymptotic stabilization to the equilibrium point can not be achieved in implementation mainly due to motor friction. Figure B.1 shows the effect of motor friction on the closed loop system behavior.

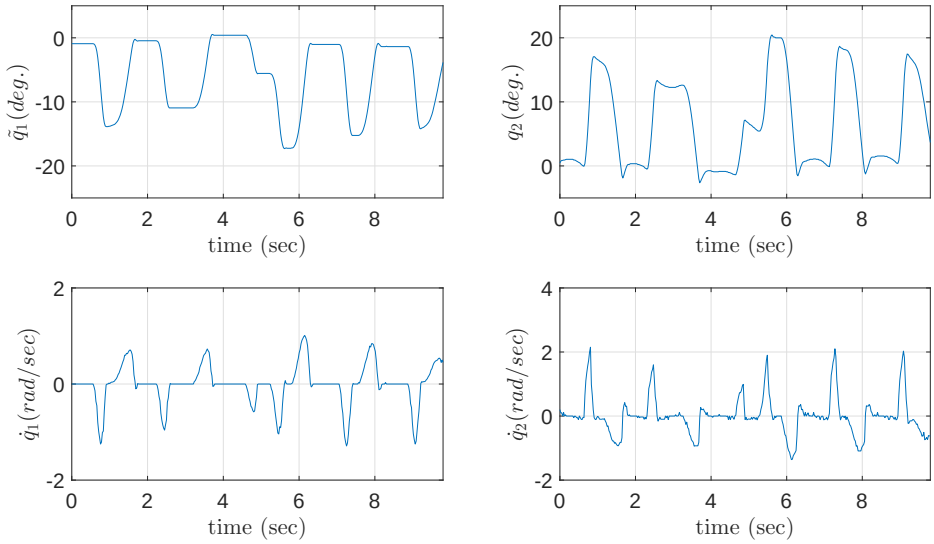

Figure B.1: Time response of states

In this case, the poles of the closed loop system (2.27) with τ in (2.31) is chosen such it has near critical damping behavior. When the linkage moves close to $\tilde{q}_1 = 0$, the torque is no longer sufficient to overpower the opposing torque due to motor friction. Hence, it stops before $\tilde{q}_1$. The Pendubot exhibits this behavior almost every time when $\tilde{q}_1$ approach 0. The motor friction introduces dead-zone in the Pendubot about the upright position. However, with different choice of poles, this behavior can be avoided and most likely, something better can be achieved. In this case, underdamped poles would help.

Before going to gain tuning, details of desired behavior of the closed loop system are given.

1. $$|x\| \leq \epsilon, \epsilon > 0 \tag{B.2}$$

   This fixes limit on joint angles and joint velocities. We expect the system to be confined within a small neighbourhood of x_{top} and it should never come out of the neighbourhood, atleast not often. In addition, the magnitude of oscillation of the states should be atleast near-stationary. If not, the system will be wobbling about the upright position.

2. The system should have good disturbance rejection.

3. The closed loop system should be robust to parameter variation, especially initial conditions $\tilde{q}_1(0)$ and $q_2(0)$.

Tuning procedure

Here, the poles of the closed loop system are tuned, instead of gain components of the gain matrix K. The main objective is to obtain the closed loop response that satisfies the conditions laid down by tuning of the poles. Our concern is to achieve desired behavior by utilizing the pole positioning to the fullest measure so we do not care whether the system can be reduced to a lower order by second-order approximation.

Let the poles of the closed loop system be $P = (p_1, -\sigma + j\omega, -\sigma + \omega, p_4)^T$. The choice of the structure of poles should be evident by now. Pole p_1 is chosen to be far away from the origin which determines the operating torque of the system. Since ζ is fixed to be between 0 and 1, it s chosen 0.5 to start with. Rise time or peak time condition on the system behavior can be used to provide good starting value for ω_n. p_4 can be chosen to be 4 or 5 times the real part of $(-\sigma + j\omega)$ for good initial guess.

The tuning rules adopted for state feedback control are listed below

1. If the Pendubot does not stay in the region, decrease the damping. Damping can be decreased by 1) increasing ω_d 2) decreasing σ 3) increasing p_4. When the Pendubot destabilizes, increase the damping.

2. If the system begins to wobble around x_{top}, then decrease p_1. This is due to high gain matrix. Note increasing p_1 aggravates the behavior of the system determined by $(-\sigma \pm j\omega, p_4)$. For example, if the damping is low for the system, then increasing p_4 destabilize the system.

B.3 Energy based approach for swing up control

The control law for energy based approach is given as

$$\tau = \frac{-k_D F(q, \dot{q}) - (P_1 P_2 - P_3^2 \cos^2 q_2)(\dot{q}_1 + k_P \tilde{q})}{(P_1 P_2 - P_3^2 \cos^2 q_2) k_E \tilde{E} + k_D P_2} \tag{B.3}$$

It has three gains namely, k_P, k_D and k_E. If the constraints (2.22) and (2.23) on the gains and initial condition are satisfied, the Pendubot will reach the homoclinic orbit.

The constraint (2.22) ensures the control law is non-singular.

$$\frac{k_D}{k_E} > 2P_1(P_4 + P_5)g \tag{B.4}$$

From the control law τ, it is clear that denominator of the control law is positive as long the constraint (2.22) is satisfied. So increasing k_E can effectively increase the control law τ. τ can be increased by decreasing k_D also.

The tuning procedure adopted to bring the Pendubot to the basin of attraction of the stabilizing controller is given below.

1. When the energy of the pendubot is saturated and no longer increasing to E_{top}, increasing the energy delivered would help the Pendubot to reach to the basin of attraction of the stabilizing controller. The energy delivered can be increased by increase in k_E , decrease in k_D or increase in k_P.
2. If the energy delivered is too high such that the linkage falls down, then decrease k_E or increase k_D.

REFERENCES

1. **Block, D. J.** (1996). *Mechanical Design and Control of the Pendubot*. Master's thesis, University of Illinois, Urbana-Champaign.

2. **Consolini, L.** and **M. Maggiore** (2011). On the swing-up of the pendubot using virtual holonomic constrains. *50th IEEE Conference on Decision and Control and European Control Conference*, **15**(1), 4803 – 4808.

3. **Fantoni, I.**, **R. Lozano**, and **M. W. Spong** (2002). Energy based control of the pendubot. *IEEE International Conference on Control Applications*, **45**(4), 725–729.

4. **Gulan, M.**, **M. Salaj**, and **B. RohalâĂŹ-Ilkiv** (). Achieving an equilibrium position of pendubot via swing-up and stabilizing model predictive control. *Journal of Electrical Engineering*.

5. **Khalil, H. K.**, *Nonlinear systems*. Prentice Hall, New Jersey, 1996.

6. **Merry, R.**, **M. van de Molengraft**, and **M. Steinbuch** (2010). Velocity and acceleration estimation for optical incremental encoders. *Mechatronics*, **20**(1), 20–26.

7. **Muralidharan, V.** (2014). *Smooth Asymptotic Stabilization of Position and Reduced Attitude for Nonholonomic Mobile Robots*. Ph.D. thesis, Department of Electrical Engineering, IIT-Madras, Chennai – 600036.

8. **Spong, M. W.** (1995). The swing up control problem for the acrobot. *IEEE Control Systems Magazine*, **15**(1), 49–55.

9. **van der Laan, M. D.** (1995). *Signal Sampling Techniques for Data Acquisition in Process Control*. Ph.D. thesis, University of Groningen, Groningen.

10. **Xin, X.**, **M. Kaneda**, and **T. Oki**, The swing up control for the pendubot based on energy control approach. *In 15th Triennial World Congress*. International Federation of Automatic Control, 2002.

11. **Xin, X.**, **S. Tanaka**, **J. She**, and **T. Yamasaki** (2013). New analytical results of energy-based swing-up control for the pendubot. *International Journal of Non-Linear Mechanics*, **52**(4), 110–118.

12. **Yabuno, H.**, **T. Matsuda**, and **N. Aoshima** (2005). Reachable and stabilizable area of an underactuated manipulator without state feedback control. *IEEE/ASME Transactions on Mechatronics*, **10**(4), 397–403.

13. **Zhang, M.** and **T.-J. Tarn** (2002). Hybrid control of the pendubot. *IEEE/ASME Transactions on Mechatronics*, **7**(1), 79–86.